The Unusual Intensity Behavior of the 281-cm^{-1} Resonance Raman Band of C_{60}: A Complex Tale of Vibronic Coupling, Symmetry Reduction, Solvatochromism, and Jahn−Teller Activity

Sean H. Gallagher,* Keiran C. Thompson, Robert S. Armstrong, and Peter A. Lay

School of Chemistry, University of Sydney, Sydney, NSW, Australia 2006

Received: September 22, 2003; In Final Form: March 30, 2004

Resonance Raman (RR) Stokes and anti-Stokes experiments were performed on C_{60} in benzene, toluene, and CS_2 solutions in the low energy region 240−300 cm^{-1} with the laser probing the first-allowed electronic transition, "A". Two bands were evident at 265 and 281 cm^{-1}, which are both assigned to *E* modes that originate from the $H_g(1)$ mode of I_h C_{60}. The 16 cm^{-1} energy separation suggests that the ground-state geometry of C_{60} in solution is significantly distorted. The solvatochromism of C_{60} was used to "tune" the laser relative to the A transition. The band at 281 cm^{-1} displays unusual intensity behavior in that it has greater intensity in the anti-Stokes region of some RR experiments relative to the Stokes region, even though thermal populations of the first vibrational excited state do not exceed 20%. Further, the 281 cm^{-1} band appears to have intensity when the incident laser is able to probe the $^1A_g \rightarrow [1T_{1u} + H_g(1)]$ vibronic transition (0−1) of C_{60}, but not when the laser is in resonance with the pure electronic transition, $^1A_g \rightarrow 1T_{1u}$ (0−0). As such, the 281 cm^{-1} band appears to have a Raman excitation profile that follows the 0−1 absorption envelope. The RR intensity of the 281 cm^{-1} band is proposed to derive from the intramanifold coupling of the A and E states, which arise from the T_{1u} electronic state under I_h symmetry, further strengthening the case that D_{5d} is a good approximation for the symmetry of C_{60} in solution.

Introduction

Probing the weakly allowed HOMO−LUMO transition of C_{60} and its vibronic sideband through resonance Raman (RR) spectroscopy opens a veritable Pandora's Box of vibronic coupling in the first and most famous member of the fullerene family. Indeed the resulting RR solution spectra of C_{60} are surprisingly rich in a manner reminiscent of the RR solution spectra of metalloporphyrins.[1−3] Many of these features arise through the solvent interaction with C_{60}. It is the nature of this interaction and its effect on the vibronic coupling of C_{60} related to the first electronic excited state that require further investigation.

Despite this wealth of RR information, many areas remain under-developed. For instance, why do some RR phenomena seem to support the labeling of I_h symmetry in solution for C_{60}, whereas others point to a lower symmetry, perhaps D_{5d}? The triply degenerate LUMO should be subject to Jahn−Teller distortion.[3−6] Why then do the RR solution spectra of C_{60} display no definitive evidence for such JT activity even though this technique is highly sensitive for probing Jahn−Teller distortions of degenerate electronic excited states?[7,8] What is the nature and extent of the solvent interaction with ground-state C_{60} and what effect does this have on electronically excited C_{60}?[2,9]

The importance of better understanding the vibronic coupling of C_{60} is related to many of its promising applications, such as superconductivity and ferromagnetism. (For a recent review on superconductivity, see ref 10.) It has even been suggested recently that certain organic functionalized C_{60} moieties could be used as novel polar liquid crystalline materials,[11] leading to applications such as photovoltaic paint. (For example, see *Science et Vie* **2003**, 1026, 20.)

There is a growing body of evidence for the lower symmetry of ground-state C_{60} in solution. This includes the intensity of forbidden electronic transitions in the absorption spectrum and also the appearance of bands due to Raman-silent modes in the solution RR spectrum. There are many plausible explanations for this symmetry reduction. For instance, the presence of a ^{13}C atom in about one in two molecules can explain some additional features in the Raman spectrum of C_{60}.[12] However, this slight perturbation in the fullerene cage cannot account for the activation and intensity of bands energetically well removed from Raman fundamental modes of C_{60} previously reported by us, including most notably the 281 and 1140 cm^{-1} RR bands.[2,3] Furthermore, the solution RR spectra of C_{60} are markedly different from the solid Raman spectra of C_{60}, where ^{13}C is the primary contributor to deviations from the predicted Raman spectrum. The answer must, therefore, lie in the nature of the solvent interaction with the fullerene cage in both the ground and excited states. Rubstov et al. suggest that in more electron donating solvents, distortions of the sphericity of the electrophilic C_{60} may occur because the "effective volume of the rotating molecule increases".[13] While this is more likely to occur in relation to the excited-state axial quadrupole where the solute−solvent interaction is more anisotropic,[9,14] such specific solute−solvent interactions are not likely to occur in the nonpolar ground state. We provide some comment on possible ground-state symmetry reduction mechanisms.

We have suggested elsewhere that the general structure of the electronic absorption spectrum and vibronic coupling of C_{60} can be compared to those of metalloporphyrins.[1,3] Recent TD-DFT results reported by Bauernschmitt et al. further support

* Corresponding author. Phone +61−2−9351−4601 (w); Fax +61−2−9351−6877; E-mail sean@chem.usyd.edu.au.

10.1021/jp036834w CCC: $27.50
Published on Web 06/03/2004

this view.[15] In their paper, the second allowed electronic transition of C_{60} ($1^1A_g \rightarrow 2T_{1u}$) was reassigned to the higher energy, strongly allowed transition at ~330 nm, originally assigned by Leach et al. as 'C'.[4] This transition will henceforth be referred to in this paper as 'B'. The first-allowed electronic transition (HOMO−LUMO), 'A' ($1^1A_g \rightarrow 1T_{1u}$), remains as originally assigned at ~410 nm and has an extended vibronic sideband of 0−1 transitions that lies in the foothills of the B transition. This is strikingly similar to the Q and B electronic transitions of metalloporphyrins, suggesting that the vibronic coupling interactions exhibited by metalloporphyrins are likely to be similar, especially in a solvent environment. (The earlier work of Shelnutt[16] on the effect of vibronic coupling on the RR spectra of metalloporphyrins in a low symmetry environment is pertinent to the discussion here.) This should not be surprising given that both fullerenes and porphyrins have fairly rigid extended networks of fused unsaturated rings. Indeed, both molecular systems display many similar types of scattering phenomena. This includes rare D-term RR scattering for C_{60}; the only known occurrence of this phenomenon outside the family of porphyrins.[1]

Although an extensive account of the RR scattering mechanisms in C_{60}, including Raman excitation profiles and solvent interactions, has been well documented,[2,3] the unusual intensity behavior of the 281 cm^{-1} band requires that the nature of the solvent interaction with C_{60}, and its effects on vibronic coupling, be revisited. The intensity behavior of the C_{60} RR band at 281 cm^{-1} is investigated in relation to the stronger 265 cm^{-1} RR band for the first time. In what is believed to be previously unreported RR scattering behavior, the 281 cm^{-1} band appears to only receive intensity under unusual resonance conditions, especially in relation to the Stokes and anti-Stokes scattering, whereas the 265 cm^{-1} band intensity exhibits more usual intensity behavior. What is at first sight an interesting spectral curiosity actually reveals important clues about the symmetry and vibronic coupling of C_{60} in solution and may be used as a more specific probe of the nature of the solvent interactions with C_{60}. We propose an assignment for this band as well as to suggest a new assignment for the 265 cm^{-1} band due to the $H_g(1)$ mode of C_{60} in a solution environment. The nature of the T_{1u} LUMO of C_{60} in the solvent environment and how this interaction relates to the 281 cm^{-1} band is also discussed.

Experimental Section

A Spectra Physics 2020 CW Kr^+ ion laser provided the violet 406.67 nm and 413.10 nm lines, hereafter referred to as 406 and 413 nm lines, respectively. Typically, powers at the laser ranged from 30 to 90 mW. The laser spot radius at the sample was 0.5 mm. The scattered light was focused with a Leitz f1.0 lens and collected at a 90° scattering geometry from the quartz spinning cell (>4000 rpm). A polarization scrambler was used in all experiments to correct for the polarization bias of the Jobin-Yvon U1000 double monochromator (1800 grooves/mm gratings). The slit setting was 300 μm for all experiments. The data were collected at 1 cm^{-1} intervals with an error of ±1 cm^{-1} across the range 240 to 300 cm^{-1} for the Stokes experiments and −240 to −300 cm^{-1} for the anti-Stokes experiments. The room temperature for each experiment was 293 K. Before each experiment, the monochromator was calibrated using the mercury emission lines of the fluorescent lights in the laboratory, for both the Stokes and anti-Stokes experiments. "Peaking up", where the signal-to-noise ratio was optimized, was performed using a strong solvent Raman band in each experiment: at 991 cm^{-1} in benzene, 1004 cm^{-1} in toluene, and 694 cm^{-1} in CS_2.

A typical experiment involved the collection of eight consecutive scans at an 8-s integration time for each datum point. The resultant spectrum was then taken from the average of the eight scans after ensuring there was no observable photodecomposition of the sample over the time scale of each experiment. All RR spectra are uncorrected for baseline, and no smoothing has been performed. Polarization experiments were performed as per normal RR experiments, but with a polarization analyzer placed between the scrambler and the collection lens.

Experiments to determine RR intensity dependence on laser power were performed in benzene using 406-nm excitation in the Stokes region. Laser powers at the sample were measured by an Ophir Optronics Nova laser power monitor with a PD300−3W (ver. 2) head. The head was placed between the focusing lens and the spinning sample and tuned to the required wavelength between 350 and 1100 nm, with an accuracy of ±0.001 mW. The laser powers at the sample for these experiments were 8.1, 16.3, and 23.8 mW. In each experiment, the relative intensities of the 265 and 281 cm^{-1} bands were compared with the intensity of the 606 cm^{-1} band of benzene. The relative intensities were uncorrected for the spectral response of the detector as there is minimal change in the response in the absolute energy region, 23982−24323 cm^{-1}, for the three bands at 406.7 nm excitation.[14]

The C_{60} used in this work was obtained from the MER Corporation. Two different purities were used (99.9% and 99.5%) in order to determine whether impurities contribute to the weak bands in the spectra. The benzene, toluene and CS_2 solvents were of spectroscopic grade (>99.9%) and were used as received. The C_{60} concentration of each solution was approximately 1.7, 2.8, and 7.9 mg/mL for the benzene, toluene, and CS_2 solutions, respectively. The carcinogenic nature of benzene and toluene required all preparations to be performed in a well-ventilated fume hood.

Deconvolution of absorption and RR spectra was performed using the curve fitting program within the Opus 3.01 software by Bruker.[17] For each curve fit, the Levenberg−Marquardt algorithm was used and each curve was fit as a Gaussian. The baseline used in RR spectra was linear while the baseline used in the electronic absorption spectra was Lorentzian to signify the long tail of strong electronic absorptions to higher energy. Eight bands were chosen to fit each of the regions between 395 and 420 nm for benzene and toluene and 398−423 nm for CS_2 based on the results of Leach et al.[4] and taking into account solvatochromic shifts.[9] Each resulting curve fit had an RMS error of <0.0025.

Results

RR spectra of C_{60} were recorded in benzene, toluene, and CS_2. The positions of the laser excitation wavelengths used (406.7 and 413.1 nm), in relation to the HOMO−LUMO transition and its vibronic sideband of C_{60} in the three solvents, are illustrated in Figure 1. The Stokes and anti-Stokes RR spectra for benzene, toluene, and CS_2 at both excitation wavelengths are shown in Figures 2−4.

In the Stokes region of 240−300 cm^{-1}, two RR bands were evident at 265 cm^{-1} and 281 cm^{-1} and in the corresponding anti-Stokes region at −265 and −281 cm^{-1}. In all RR experiments, the band at 265 cm^{-1} was evident. In contrast, the band at 281 cm^{-1} appeared under certain energy conditions: in benzene and toluene in the 413.1 nm anti-Stokes experiments and 406.7 nm Stokes experiments; in CS_2 in the Stokes and anti-Stokes experiments at 413.1 nm. The 281 cm^{-1}

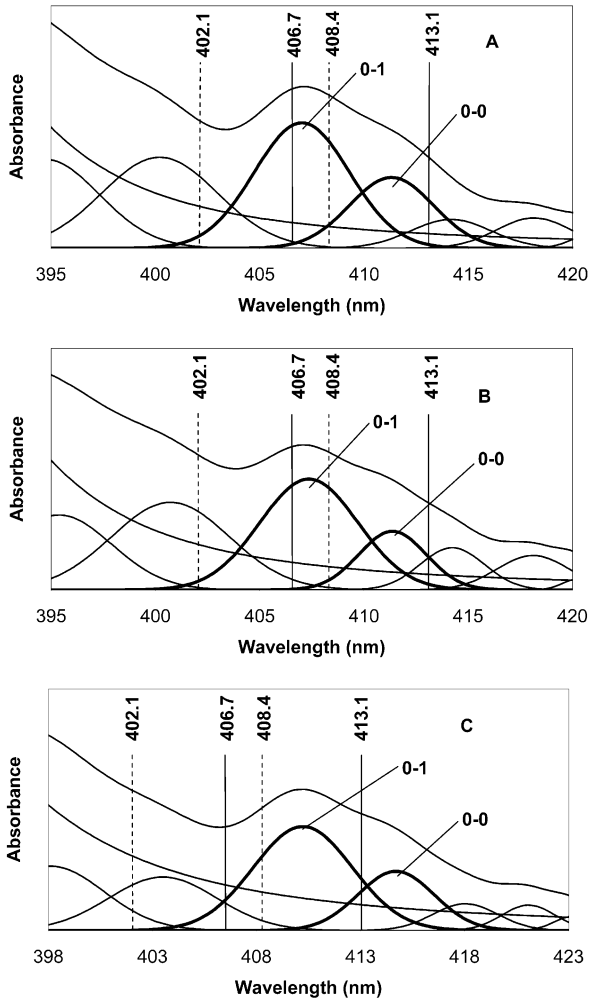

Figure 1. Deconvolution of electronic absorption spectra of C_{60} at 20 °C, showing the positions of the 413.1 and 406.7 nm laser lines relative to the A electronic transition. The dashed lines at 408.4 and 402.1 nm represent the energy conditions of the 413.1 and 406.7 nm lines, respectively, in the anti-Stokes experiments for the first vibrational excited state of the 281 cm^{-1} band in the ground electronic state: (A) benzene 395−420 nm, (B) toluene 395−420 nm, (C) CS_2 398−423 nm. Each spectrum has been deconvoluted into component absorption bands as per the assignment of Leach et al.[4] The 0−0 band refers to the origin transition and the 0−1 band is due to the first vibronic transition involving the $H_g(1)$ mode.

band was barely discernible in the 413.1 nm Stokes experiment in benzene and toluene and in the 406.7 nm Stokes experiment in CS_2 (see insets in Figures 2a, 3a, 4c).

The depolarization ratios for both the 265 and 281 cm^{-1} bands were recorded and are given in Table 1. The depolarization ratios for the bands of the two totally symmetric A_g modes of C_{60} at 490 and 1468 cm^{-1} were also recorded for comparison purposes and to help determine the extent of dispersion effects. Variable laser power experiments were performed and are recorded in Table 2.

Discussion

There are four questions that arise regarding the presence of the 281 cm^{-1} RR band of C_{60} that are of interest and will be addressed in this paper: (1) What is the origin and nature of the 281 cm^{-1} band and its relation to the 265 cm^{-1} band, hereto assigned to the $H_g(1)$ squashing mode of C_{60}? (2) Under what laser resonance conditions does the 281 cm^{-1} band appear and what role does the solvent play? (3) By which scattering mechanism does the 281 cm^{-1} band receive its intensity and why does it appear only under unusual energy conditions? (4) What is the symmetry of C_{60} in solution?

Origin of 281 cm^{-1} Band. If much significance is to be placed on the appearance of an unexpected weak RR band at an unexpected position under unexpected conditions, then it is imperative to demonstrate as thoroughly as possible not only its likely origin but also what it is not.

The assignment of the 281 cm^{-1} band to an electronic ground-state vibrational mode of C_{60} can be made for many reasons. First, this band appears in both the Stokes and anti-Stokes RR experiments for C_{60}. Second, we have used different purities of C_{60} (99.5% and 99.9%) from the same source in the experiments. As there is half an order of magnitude difference in the concentration of impurities, with no observable difference in the relative intensity of the 281 cm^{-1} band in the resulting spectra, it does not appear to be impurity related. Third, the band appeared in experiments using different solvents and thus is not due to a solvent Raman band. Fourth, this band was also evident in previously reported work, which used C_{60} from a different source and thus is not source-related.[2,3] Fifth, the intensity of the band does not change over the time scale of the experiments (1−2 h) and thus is not due to the product of a chemical or photochemical decomposition reaction.

Power dependence experiments were also performed to ascertain whether the intensity of the 281 cm^{-1} band was dependent on the intensity of the laser, relative to the intensities of a C_{60} RR band and benzene solvent Raman band. The purpose of these experiments was to help determine whether the presence of the 281 cm^{-1} band was an excited-state Raman effect. The relative intensities of the 281 cm^{-1} band at 8.1, 16.3 and 23.8 mW of power (406 nm excitation) at the sample were the same, within experimental error, in comparison with those of the 265 cm^{-1} RR band of C_{60} and the 606 cm^{-1} Raman band of benzene (Table 2). With a spot radius of 0.5 mm, these laser powers equate to a laser flux ranging from 0.13 to 0.40 W cm^{-2}, well below the value of 4×10^3 W cm^{-2} reported by Chambers et al. as being required to produce a significant triplet state population.[18] Further, the Raman spectroscopic signature of the molecular triplet state of C_{60} has been assigned to a band at 1466 cm^{-1}, which is the softening of the band due to the $A_g(2)$ mode at 1469 cm^{-1}. No band at 1466 cm^{-1} is evident in this work and excited-state Raman effects are eliminated as a source for the 281 cm^{-1} band.

It is important to also make a comment on the photodecomposition work reported by Chambers et al.[18] They reported that C_{60} could be photopolymerized from solutions of chlorobenzene and toluene. After irradiating the solution with a laser power of 50 mW, an insoluble deposit formed on the surface of the cuvette and that the frequency of the band due to the pentagonal pinch mode of C_{60} softened from 1469 cm^{-1} to 1458 cm^{-1}. The conditions in the experiments reported here differ in two important ways. A spinning cell was used and the intensity of the laser at the sample was 3 orders of magnitude lower. As a result, there was no apparent buildup of any insoluble material nor was there any change in the frequency of the band due to the pentagonal pinch mode. Thus, the experimental conditions used here appeared to avoid producing such a photochemical product.

Dimerization of C_{60} must also be addressed. A report on the Raman scattering of powdered samples of C_{120} by Lebedken et al.[19] revealed a number of unique spectral signatures of C_{120}. These include the band due to the $A_g(2)$ pentagonal pinch mode softening to 1463 cm^{-1} and the removal of degeneracy of the $H_g(1)$ mode, evidenced by three bands at 258, 270, and 296

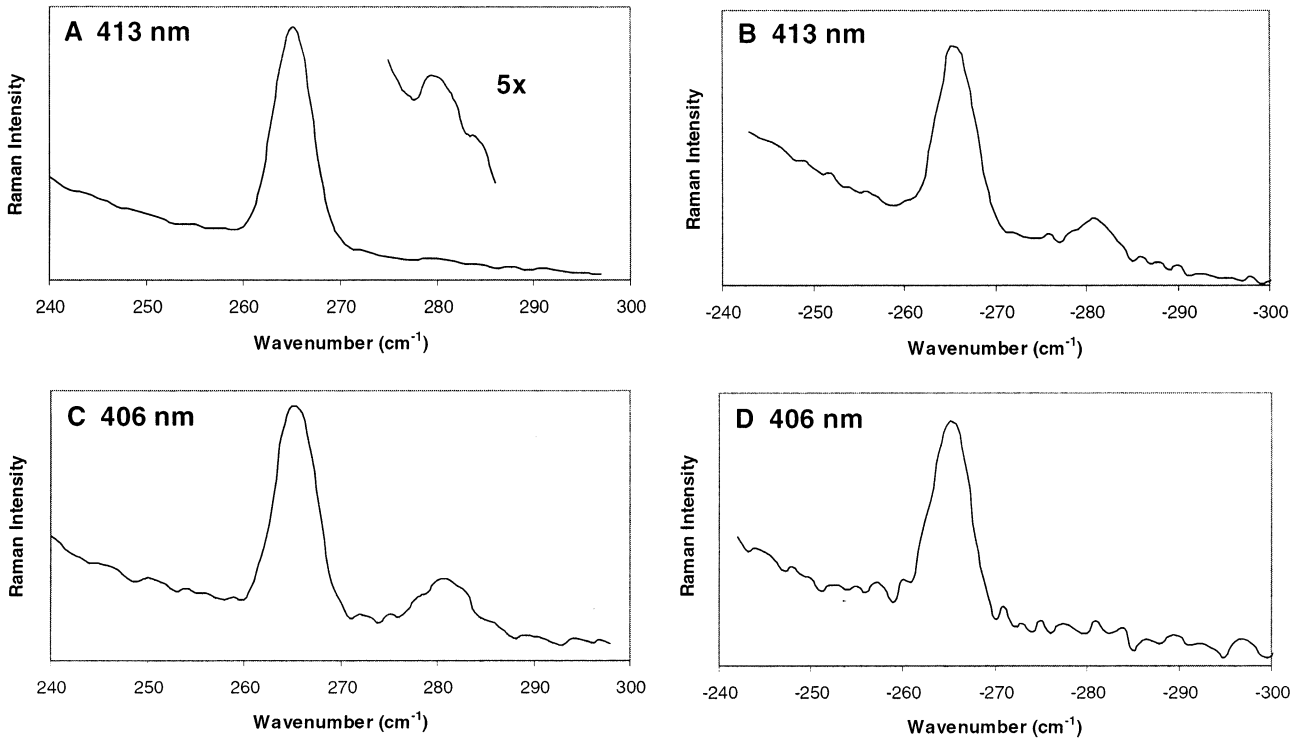

Figure 2. RR spectra of C_{60} in benzene at 20 °C: (A) 413 nm excitation Stokes, (B) 413 nm excitation anti-Stokes, (C) 406 nm excitation Stokes, (D) 406 nm excitation anti-Stokes.

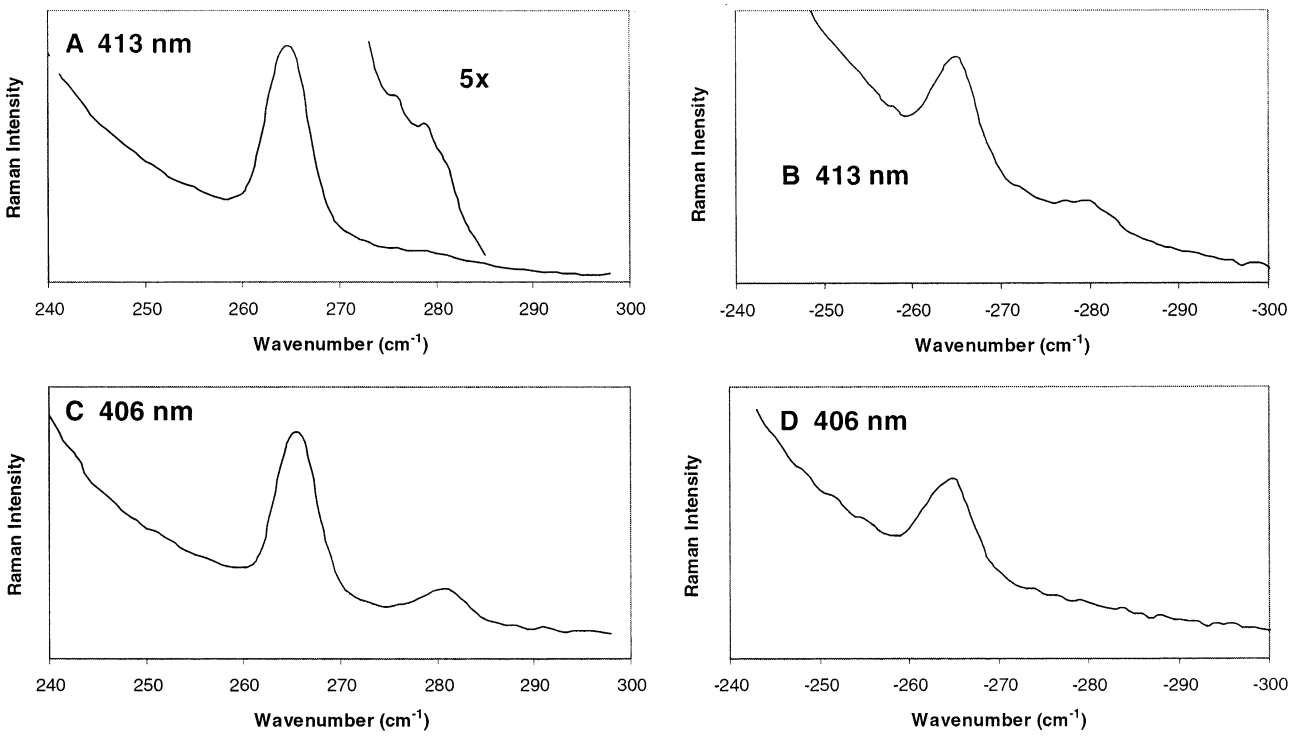

Figure 3. RR spectra of C_{60} in toluene at 20 °C: (A) 413 nm excitation Stokes, (B) 413 nm excitation anti-Stokes, (C) 406 nm excitation Stokes, (D) 406 nm excitation anti-Stokes.

cm^{-1}. They also showed that the Raman spectrum of photo-transformed C_{60} has similar characteristics in the low energy region to the three aforementioned bands. Based on these reports, there is no evidence in the RR spectra in the current work of the presence of C_{120} through dimerization of C_{60} and thus it is eliminated as a source for the 281 cm^{-1} band.

The presence of oxygen in these high energy experiments could conceivably cause oxidation of the fullerene cage. Krause et al.[20] reported on the vibrational signatures of fullerene oxides, specifically $C_{60}O$, $C_{120}O$, and $C_{120}O_2$. In $C_{60}O$, the degeneracy of the $H_g(1)$ mode is removed, producing four bands at 247, 259, 268, and 289 cm^{-1}. The three lowest energy bands overlap, producing a broad envelope; the highest energy band has very weak intensity. The band due to the pentagonal pinch mode in $C_{60}O$ is red shifted to 1464 cm^{-1}. In the Raman spectra of $C_{120}O$ and $C_{120}O_2$, seven and 10 bands, respectively, are evident due

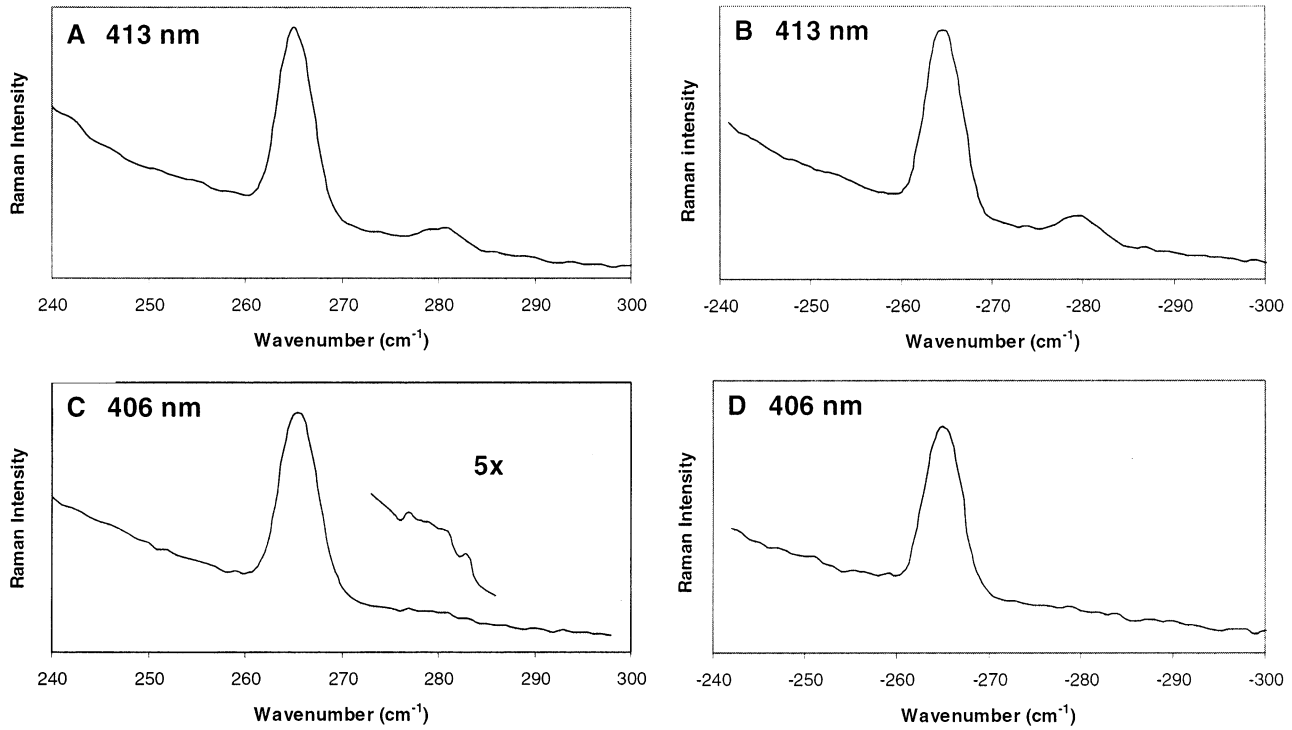

Figure 4. RR spectra of C_{60} in CS_2 at 20 °C: (A) 413 nm excitation Stokes, (B) 413 nm excitation anti-Stokes, (C) 406 nm excitation Stokes, (D) 406 nm excitation anti-Stokes.

TABLE 1: Depolarization Ratios for the Bands at 265, 281, 490, and 1468 cm^{-1} for C_{60} in Benzene in the Stokes RR Experiments

band (cm^{-1})	413.1 nm	406.7 nm
265	0.73 ± 0.10	0.67 ± 0.10
281	n/a	0.47 ± 0.30
490	0.00 ± 0.01	0.00 ± 0.01
1468	0.05 ± 0.01	0.07 ± 0.01

TABLE 2: Relative Intensities of the 265 and 281 cm^{-1} Bands of C_{60} Compared with the 606 cm^{-1} Band of Benzene at Three Different Laser Power Settings at 406 nm Excitation[a]

band (cm^{-1})	8.1 mW	16.3 mW	23.8 mW
265	0.019	0.018	0.019
281	0.004	0.005	0.005
606	1.000	1.000	1.000

[a] The error in relative band intensity is ± 0.001.

to the reduction in the symmetry of the $H_g(1)$ mode and the pentagonal pinch mode lies at 1464 cm^{-1} for both dimers. As the Raman features for these oxidized fullerenes are phenomenologically different from the results reported here, oxidation can also be discounted.

There have been several reports in the literature about the aggregation of C_{60} in solution. In one of the earliest, Ying et al.[21] reported that C_{60} can form unstable aggregates with a "loose structure" in benzene, held together weakly by van der Waals forces. The aggregation is reversible simply by shaking the solution. Rudalevige et al. showed similar behavior with C_{60} reversibly aggregating in benzene solution (1 mM) over several days.[22] However, more recently, Nath et al.[23] have demonstrated that an equilibrium exists in solution between C_{60} aggregates with isolated C_{60} molecules only in polar solvents. The dielectric constant of the solvent (ϵ) needs to be greater than 13 for aggregation to occur in a concentrated solution. In aromatic solvents such as benzene ($\epsilon = 2.28$), C_{60} existed only as a monomer in solution. This result is consistent with previous work that showed that the dielectric properties of a solvent must be considered in determining the absorption characteristics of C_{60} in solution.[9] Even if there were a slight possibility of aggregation of C_{60} in solvents such as benzene, toluene, and CS_2, these reports in the literature suggest that any such aggregation would be both solvent- and time-dependent. Neither of these variables altered the presence and reproducibility of the spectral response of the 281 cm^{-1} band. In any case, it is highly probable that any C_{60} aggregate would be easily broken up in a cell spinning at >4000 rpm.

The nearest Raman fundamental mode for C_{60} has been assigned in the literature to the band due to the non-totally symmetric $H_g(2)$ mode at 427 cm^{-1}. As this band is energetically well separated from the 265/281 cm^{-1} "doublet", symmetric reduction of the $H_g(2)$ mode is eliminated as a source for the 281 cm^{-1} band. In terms of other C_{60} fundamental vibrational modes, Hara and co-workers[24] performed DFT calculations, which showed good agreement in the low energy region between calculated and experimental results. Out of the 46 fundamental vibrational modes of I_h C_{60}, only one was in the 200−300 cm^{-1} region, which was a peak at 269 cm^{-1} and assigned to the $H_g(1)$ mode. The next fundamental vibrational frequency was due to the $T_{2u}(1)$ mode, with a calculated peak at 343 cm^{-1}.[25]

This result is supported more recently by Schettino et al.,[26] who performed DFT calculations of the vibrational frequencies. Only one fundamental vibrational frequency was predicted to exist below 300 cm^{-1}, the $H_g(1)$ mode. Like Hara et al., Schettino et al. calculated the next vibrational frequency to be the $T_{2u}(1)$ mode with a peak at 342 cm^{-1}. Schettino et al. reported that the presence of other bands in the region of the bands of fundamental modes of C_{60} are either due to symmetry lowering effects of ^{13}C or crystal effects, or perhaps both. That is, these additional bands in this region are not due to icosahedral fundamental vibrational modes themselves. It is, therefore, necessary to discuss reports of the presence of other bands in the region of the $H_g(1)$ mode. In many papers, two bands are

reported in the region of the band of the $H_g(1)$ mode. In the Raman spectra of solid or crystalline C_{60}, the band of the $H_g(1)$ mode at 271 $\pm$1 cm^{-1} is reported together with another band at 265 $\pm$1 cm^{-1} by several researchers.[27−29] Choi et al. and Martin et al. report that both bands derive from the same H_g fundamental mode and that the lower energy band does not derive from a solvated C_{60}. Given that the position of the band of the $H_g(1)$ mode is at 265 cm^{-1} of C_{60} in solution in the work reported here, this is an unlikely explanation. However, we concur with their conclusion, which is further supported by the Raman spectroscopic studies of Talyzin et al.[30] on C_{60} solvates. Talyzin et al. showed that the band of the $H_g(1)$ mode was found at 269 cm^{-1} in a range of C_{60} solvates.

Despite this evidence for the existence of two bands in this region of the spectrum, the greatest reported energy difference between them in solid C_{60}, thin films, or C_{60} solvates is around 6 cm^{-1}, which is significantly less than the 16 cm^{-1} difference reported here. To put this energy splitting in perspective, it is important to consider four unrelated results. In the RR spectrum of the heterofullerene dimer $(C_{59}N)_2$,[31] the band due to the $H_g(1)$ mode appeared to be split into a doublet with peaks at 271 cm^{-1} and 286 cm^{-1}, Δ = 15 cm^{-1}. The relative intensities of the two bands are similar to those reported here for the 265 and 281 cm^{-1} bands. Second, Chen et al. reported the Raman spectra of solid Ba_xC_{60}, where x = 3, 4, 6.[32] For both Ba_3C_{60} and Ba_6C_{60}, two bands were reported as corresponding to a reduction in symmetry of the $H_g(1)$ mode, with energy separations of 6 and 7 cm^{-1}, respectively. However, in the Raman spectrum of Ba_4C_{60}, four bands, with a maximum energy difference of 32 cm^{-1}, were assigned to bands that arise from a reduction in symmetry of the $H_g(1)$ mode. They attributed this splitting to the symmetry lowering of C_{60} due to the orthorhombic structure of this material and make reference to a similar result observed in single-crystal K_3C_{60} at 80 K, in which the bands arising from the $H_g(1)$ mode are separated into five components.[33] Third, in the surface-enhanced Raman spectrum of C_{60} adsorbed onto gold, the degeneracy of the $H_g(1)$ mode was removed, producing two bands at 256 and 270 cm^{-1}, Δ = 14 cm^{-1}.[34] Fourth, the FT-Raman spectrum of $[Ru(NH_3)_5(\eta^2{-}C_{60})](CF_3SO_3)_2$, where the ruthenium is bonded to two C_{60} carbons, revealed two bands at 271 and 287 cm^{-1}, a difference of 16 cm^{-1}.[35]

On the balance of the evidence above, the presence of two bands in this region due to C_{60} is not entirely unexpected. Thus we assign the 265 and 281 cm^{-1} bands as deriving from the $H_g(1)$ fundamental mode of C_{60}. In contrast, the energy difference between them seems uncharacteristically large for pure C_{60}, suggesting that the ground-state symmetry of C_{60} in the solvent environment is significantly reduced.

Assignment of the 281 cm^{-1} Band. The depolarization ratios, $\rho(\pi/2)$, of the 265 and 281 cm^{-1} bands were measured to help identify the symmetries of these modes. For a cubic molecule such as C_{60}, $\rho(\pi/2)$ = 0 or 3/4 for totally and non-totally symmetric modes, respectively. The value $\rho(\pi/2) = I_\perp/I_{||}$, where $I_\perp$ and $I_{||}$ are the RR band intensities for the scattered light in perpendicular and parallel polarizations, respectively.[36]

The band at 265 cm^{-1} has $\rho(\pi/2)$ = 0.73 $\pm$ 0.10 at 413.1 nm excitation and 0.67 $\pm$ 0.10 at 406.7 nm. Hence, this band derives from a non-totally symmetric mode, and has been assigned previously in the literature to the $H_g(1)$ squashing mode of C_{60}. The $\rho(\pi/2)$ value for the band at 281 cm^{-1} was measured at 0.47 $\pm$ 0.30. With such a large range in experimental error, $\rho(\pi/2)$ could be anywhere between 0.17 and 0.77. However, in the $I_\perp$ experiment, the signal−noise is low at 2:1 due to the weak intensity of the 281 cm^{-1} band, exacerbated by the polarizer filter. In contrast, the signal−noise for $I_{||}$ is 5:1. Hence, the loss of signal−noise is much greater in the $I_\perp$ experiment and $\rho(\pi/2)$ for the 281 cm^{-1} band is more likely to be greater than 0.47 than less. As this value would then approach 3/4, we assign the 281 cm^{-1} band to a non-totally symmetric mode.

TABLE 3: Correlation Table for Icosahedral Symmetry for H_g Vibrational and T_{1u} Electronic Modes

I_h	D_{5d}	D_{3d}
H_g	$A_{1g} + E_{1g} + E_{2g}$	$A_{1g} + 2E_g$
T_{1u}	$A_{2u} + E_{1u}$	$A_{2u} + E_u$

C_{70} is a useful guide as to the effects of symmetry lowering on a lower symmetry species related to C_{60}. C_{70} belongs to the D_{5h} point group and is formed by inserting a band of 10 carbons between the two hemispheres of C_{60}. Onida et al.[37] have assigned three low-energy bands of this molecule in the Raman spectrum that correspond to the 5-fold degenerate $H_g(1)$ squashing mode of C_{60}. The E_2', E_1'', and A_1' modes in C_{70} have RR bands at 223, 250, and 257 cm^{-1}, respectively, as evidenced in C_{70} RR experiments in benzene.[38] This result correlates to relevant subgroups of I_h, and is found in Table 3.

Hence, in D_{5d} and D_{3d} point groups, the 5-fold degeneracy of an H_g mode is removed to become an A mode and two E modes. Thus for C_{60} in solution, we propose to assign both the 265 and 281 cm^{-1} bands to non-totally symmetric E modes in either D_{5d} or D_{3d} point groups.

Excited-State Energy Window. The intensity behavior of the 281 cm^{-1} band is not simply a question of resonance with an excited electronic state. Considering only the benzene Stokes experiments, the intensity of the 265 cm^{-1} band in each experiment are of the same of order of magnitude at 413 nm excitation and at 406 nm excitation, i.e., in resonance with the 0−0 and 0−1 transitions of the A electronic transition, respectively (Figure 2a and 2c). In contrast, the 281 cm^{-1} band was more than an order of magnitude more intense at 406 nm excitation than at 413 nm excitation (cf. Figure 2a and 2c). Similar results were recorded in toluene (Figure 3a and 3c). However in CS_2, in comparison with the 265 cm^{-1} band, the band at 281 cm^{-1} was considerably more intense at 413 nm excitation than at 406 nm excitation (Figure 4a and 4c). Unusual intensity differences between the 406 and 413 nm excitations were also evident for the 281 cm^{-1} band relative to the 265 cm^{-1} band in the anti-Stokes region (Figure 4a and 4b). Nor is the intensity behavior of the 281 cm^{-1} band simply a question of anti-Stokes scattering arising from thermal population of an excited vibrational state in the ground electronic state.[1] (Bands appear in the anti-Stokes region of the Raman or RR spectrum of a molecule when there is a significant population of molecules in the vibrational excited states for the vibration in question, with the inelastically scattered photon returning the system to a lower (usually the ground) vibrational state.) At 20 °C, the bands at 265 and 281 cm^{-1} have thermal populations in the first excited vibrational state of around 20%. Indeed, the anti-Stokes RR intensities for the 265 cm^{-1} band were not insignificant and ranged from 10 to 20% of those in the Stokes experiments, consistent with the thermal population. In fact, the thermal population of molecules in the vibrational excited state at 265 cm^{-1} would be slightly greater than that for the 281 cm^{-1} band at the same temperature, yet the anti-Stokes RR intensities for the 281 cm^{-1} band are significantly greater in many cases than their Stokes equivalents (cf. Figures 2a and 2b, 3a and 3b). As such, the greater intensity of the 281 cm^{-1} band in some anti-Stokes experiments compared with the intensity in the corresponding Stokes experiments cannot be explained through thermal population alone.

A better explanation for the intensity behavior of the 281 cm^{-1} band is that it only appears to have intensity when the laser is able to probe a well-defined excited-state energy window of C_{60}. While the same laser resonance conditions exist in the Stokes and corresponding anti-Stokes experiments with respect to the absorption spectrum, the energy conditions are different as the laser is able to probe 281 cm^{-1} higher in energy into the excited state in the anti-Stokes experiments, relative to the 281 cm^{-1} band. Thus in considering the resonance enhancement of the 281 cm^{-1} band intensity, the 413 and 406 nm excitations in the anti-Stokes experiments could be considered as the energy equivalents of using laser lines at 408.4 nm (24488 cm^{-1}) and 402.1 nm (24869 cm^{-1}), respectively, again relative to the 281 cm^{-1} band.

Closer inspection of the deconvolutions of the electronic absorption solution spectra for C_{60} in this region (Figure 1a, 1b, 1c) shows that the intensity of the 281 cm^{-1} band appears to follow the absorption envelope for the 0−1 vibronic transition, i.e., $1^1A_g \rightarrow [1T_{1u} + H_g(1)]$. Take, for example, the 413 nm excitation experiment in benzene where the 281 cm^{-1} band has very weak intensity in the Stokes region. The resonance conditions show that while the 413 nm line is clearly in resonance with the 0−0 transition, it also appears to just probe the low energy tail of the 0−1 absorption. In contrast, the intensity of the 281 cm^{-1} band is much stronger in the corresponding anti-Stokes region where the resonance conditions in energy terms are equivalent to using a 408.4-nm laser (see dashed line in Figure 1a). This is energetically closer to peak resonance with the 0−1 transition than the 413 nm line and consistent with the intensity enhancement of the 281 cm^{-1} band. Likewise, the intensity of the 281 cm^{-1} band is strongest at 406 nm excitation for the Stokes experiment, almost at peak resonance with the 0−1 transition. In the anti-Stokes experiment at 406 nm, the 281 cm^{-1} band is not evident, despite the energy conditions at 402.1 nm appearing to be in resonance with the high energy tail of the 0−1 absorption envelope. However, with the combination of the lower intensities for anti-Stokes scattering at room temperature and much lower laser powers used at 406 nm than at 413 nm, it is possible that any band intensity is lost to the noise (see Figure 2d).

In summary, by use of a combination of the solvatochromism of C_{60} in these solvents, as well as recording the anti-Stokes spectra, the laser is "tuned" relative to the A transition. Evidently, the 281 cm^{-1} band appears to have a Raman excitation profile (REP) that follows the absorption envelope of the $1^1A_g \rightarrow [1T_{1u} + H_g(1)]$ transition.

C_{60} in a Solvent Environment. The observation of the 281 cm^{-1} band in the RR spectrum of C_{60} is the manifestation of lower symmetry in both the ground and excited states. That it exists is a ground-state effect; that it has intensity is an excited-state effect. While it appears that the origin of this band derives from the degeneracy removal of the $H_g(1)$ mode in a symmetry-reduced C_{60} in the ground state, the mechanism for this lower symmetry is not immediately evident.

The answer must somehow lie in the nature of the C_{60} solvent interaction. There is mounting evidence that symmetry of ground-state C_{60} is lower in solution compared to solid, including[1−3] (i) all bands due to Raman fundamental modes soften, some up to 11 cm^{-1}; (ii) the Raman activation of IR-active and Raman-silent modes; and (iii) the degeneracy removal of some non-totally symmetric modes. As these phenomena are independent of the choice of solvent within a range of organic solvents used, and are not related to ^{13}C effects,[2,3] intuitively, C_{60} appears to attain a more energetically favorable lower symmetry configuration in solution. This lower symmetry in solution would remove the degeneracy of the $H_g(1)$ mode.

RR spectroscopy is useful in determining changes in electronic degeneracy as the depolarization ratios of totally symmetric modes are particularly sensitive to the degeneracy of the resonant electronic excited state. For I_h, indeed for all cubic point groups, the depolarization ratio for totally symmetric modes when in resonance with the triply degenerate allowed electronic excited state is 0. There is no inherent dispersion in the depolarization ratio in I_h symmetry,[39] so the dispersion displayed in the $\rho(\pi/2)$ value for the band due to the $A_g(2)$ mode arises from the lower symmetry of C_{60} in the solvent environment. At 413 and 406 nm excitation, $\rho(\pi/2)$ was 0.05 and 0.07, respectively, for the band of the $A_g(2)$ mode, while $\rho(\pi/2)$ is 0.00 for the band due to the $A_g(1)$ mode at both laser excitations.

Group theory can help explain this behavior. The depolarization ratio is influenced by the symmetry of the distortion of the molecule.[16] C_{60} most likely distorts along H_g coordinates, but certainly along non-totally symmetric coordinates, in lowering symmetry from I_h to D_{5d}/D_{3d}. This gives rise to the direct product $A_g \otimes H_g = H_g$. Thus, for a totally symmetric mode, the value of $\rho(\pi/2)$ will be influenced by the non-totally symmetric distortion and will be nonzero. The depolarization ratio will, therefore, have a value in the range $0 < \rho(\pi/2) < 3/4$, depending on the extent of distortion along the H_g coordinates. The value of $\rho(\pi/2)$ for the band due to the $A_g(2)$ mode suggests that the distortion along the non-totally symmetric H_g coordinates is small but not insignificant. In contrast, the value of $\rho(\pi/2)$ band due to the $A_g(1)$ mode does not display such dispersion.

It appears, therefore, that the vibrational degeneracy of the H_g mode is more sensitive to perturbations from the solvent environment than is the electronic degeneracy of the T_{1u} mode. This suggests that there is likely to be only a small difference in energy between the I_h and lower symmetry species of C_{60}. In pure I_h symmetry, the potential energy surface, with vibronic coupling included, will have six D_{5d} wells of the same energy. In theory, tunneling between the (equivalent) wells will restore the I_h symmetry. However, a small lower symmetry perturbation, such as the solvent interaction, can lower some of the wells relative to the others. As they are no longer equivalent, the resultant states will not have I_h symmetry, and the observed bands will be split.[40]

RR Scattering Mechanisms and Intensity Behavior. In terms of group theory, the C_{60} modes that can vibronically couple the T_{1u} excited electronic states are those present in the direct product. For the icosahedral point group, $T_{1u} \otimes T_{1u} = A_g \oplus [T_{1g}] \oplus H_g$. The A_g and H_g modes are Raman active (whereas the T_{1g} vibration is part of the anti-symmetrized product and is not Raman allowed). On resonance with the A electronic transition, the A_g and H_g modes couple the resonant excited state with that of the B transition of C_{60}, as evidenced by the RR intensity enhancement of the bands for all 10 Raman-active modes.[3]

Upon resonance with the A electronic transition, only the B electronic transition needs to be considered. This is an assumption based purely on energy considerations—coupling with higher electronic excited states can be neglected as they are significantly energetically removed. For instance, the energy difference between the A and B transitions is around 5500 cm^{-1}, however, the difference between the A and C transitions (third allowed electronic transition, T_{1u} symmetry) is around 13 400 cm^{-1}.[4,15] Similarly, coupling to the higher electronic states can also be discounted. Vibronic coupling to the lower-energy

orbitally forbidden singlet → triplet transitions is also unlikely because of symmetry and energy considerations.

The case for intramanifold coupling must also be considered as the T_{1u} states are triply degenerate and the symmetric direct product transforms as $T_{1u} \otimes T_{1u} = A_g \oplus H_g$. Only the 5-fold degenerate H_g modes are capable of removing the degeneracy of the T_{1u} modes, i.e., they are candidates for Jahn−Teller (JT) activity.

Why does the 281 cm^{-1} band appear only under certain energy conditions that do not apply to the 265 cm^{-1} band, especially if they derive from the same fundamental mode? The most obvious answer is that they are of different symmetries and thus couple different excited states. This seems to imply that D_{5d} is the better approximation for the ground state, as under the D_{3d} symmetry point group the $H_g(1)$ mode transforms into two non-totally symmetric *E* modes of the same symmetry (Table 3). Indeed, this supports our earlier hypothesis that D_{5d} is the best descriptor for C_{60} ground-state symmetry.[3]

It is worth highlighting what appears to be more than an interesting coincidence. The 281 cm^{-1} band, which is likely to be a result of the degeneracy removal of the $H_g(1)$ mode, only has intensity when the laser can probe the 0−1 transition, i.e., the $1T_{1u} + H_g(1)$ state, in which the electronically excited fullerene cage distorts along $H_g(1)$ coordinates.

Clearly, the 281 cm^{-1} band does not follow the Raman excitation profiles displayed by the ten Raman fundamental modes of C_{60}, and is not effective in vibronically coupling the A and B electronic excited states. However, extrapolating from the idea that C_{60} distorts along H_g coordinates in the excited state at 0−1 resonance, we propose that the E mode that gives rise to the 281 cm^{-1} band is effective in the intramanifold coupling of the resonant T_{1u} state. From Table 3, T_{1u} transforms to $A_{2u} + E_{1u}$ in D_{5d} symmetry and $A \otimes E = E$. This assumption suggests that the $1T_{1u}$ state further distorts along the coordinates of the E mode of the 281 cm^{-1} band. This in fact is not dissimilar to the band intensity enhancement of a mode involved in a JT distortion.[3]

The JT activity of the $H_g(1)$ mode is discussed in more detail elsewhere,[3] however, an additional comment is warranted. Bands of modes that are capable of lifting the degeneracy of the resonant electronic state have their RR intensities enhanced through Jahn−Teller activity. The $H_g(1)$ mode is predicted to be the most active JT mode.[5] As the solvent has already lowered the symmetry of C_{60}, it has thus facilitated the degeneracy removal of the resonant T_{1u} state into the $A_{2u} + E_{1u}$ components in D_{5d}. However, as this separation is only small, the A_{2u} and E_{1u} states probably further separate energetically along the coordinates of the E mode of the 281 cm^{-1} band.

Previous work by us on the Raman excitation profile work on C_{60} in benzene solutions appears to further support this view.[3] A characteristic of RR scattering for non-totally symmetric modes is that the band intensity of the coupling mode is equal for resonance with both 0−0 and 0−1 absorption maxima.[39] However, the REPs revealed that the 265 cm^{-1} band (deriving from the $H_g(1)$ vibrational mode) had a relative intensity at 0−1 resonance (406 nm excitation) that was lower by approximately 20% than that at 0−0 resonance (413 nm excitation).[3] In fact, referring to Table 2, the intensity of the band at 281 cm^{-1} was 25% of the intensity of the 265 cm^{-1} band at 0−1 resonance. Hence, the 281 cm^{-1} band intensity appears to account for the "lost" intensity of the 265 cm^{-1} band. As the RR intensity of the 281 cm^{-1} band at 0−0 resonance is zero and the relative intensity of the 265 cm^{-1} band is greater at 0−0 than 0−1, it would seem that the intensity of the 281 cm^{-1} band derives from the distortion of the excited state along $H_g(1)$ coordinates at 0−1 resonance.

Finally, some thoughts on the nature of the solvent-induced distortion of ground-state C_{60} are offered. On the RR time scale, the distortion of C_{60} is most likely static. Rapidly rotating, C_{60} can be considered akin to a spinning top. Hence, the solute−solvent interactions at the poles will be slightly different to those at the equator. At the equator, we postulate that these interactions have three potential components: (i) a weakening of the solute−solvent interaction due to the centrifugal force; (ii) lateral solvent movement over the surface around the equator of C_{60} by the drag caused between solvent molecules in the first coordination sphere colliding with those in the second coordination sphere; and (iii) disruption of the second coordination sphere by such collisions. This effect would be the same within experimental error for different types of solvent molecules "bound" at the equator compared to the poles. This is because the solvation at the equator is dominated by hydrodynamic effects compared to the poles where it is dominated by diffusion and surface/solute interactions.

Conclusion

Resonance Raman (RR) Stokes and anti-Stokes experiments were performed on C_{60} in organic solvents in resonance with the first-allowed electronic transition, 'A'. Partly based on depolarization ratios, the two bands evident at 265 and 281 cm^{-1} are both assigned as being due to E modes that originate from the $H_g(1)$ mode of I_h C_{60}. The 16 cm^{-1} energy separation suggests that the ground-state geometry of C_{60} in solution is significantly distorted, especially in comparison with energy differences of this doublet in other reduced symmetry environments.

The 281 cm^{-1} band appears to have a Raman excitation profile that follows the 0−1 absorption envelope and, as such, the RR intensity of the 281 cm^{-1} band is proposed to derive from the intramanifold coupling of the A and E states, which make up the former T_{1u} electronic state under I_h symmetry. The case for D_{5d} being a good approximation for the symmetry of C_{60} in solution is further strengthened.

This unusual intensity behavior of the 281 cm^{-1} RR band of C_{60} further adds to the unusual RR scattering characteristics of C_{60} in solution. Indeed, the results reported here build on our previous work in this area and shed new light on the nature of C_{60} in both ground and excited states. While it can be stated with confidence that the symmetry of ground-state C_{60} in solution is reduced significantly, the mechanism by which this occurs is not yet clear. Currently, we are continuing to investigate the nature of the solvent−solute interaction, including performing theoretical calculations.

Acknowledgment. The authors acknowledge the support from the Australian Research Council (Large and IREX to R.S.A. and P.A.L.), and an ARC Professorial Fellowship for P.A.L.

References and Notes

(1) Gallagher, S. H.; Armstrong, R. S.; Lay, P. A.; Reed, C. A. *J. Am. Chem. Soc.* **1994**, *116*, 12091−12092.

(2) Gallagher, S. H.; Armstrong, R. S.; Lay, P. A.; Reed, C. A. *Chem. Phys. Lett.* **1996**, *248*, 353−359.

(3) Gallagher, S. H.; Armstrong, R. S.; Clucas, W. A.; Lay, P. A.; Reed, C. A. *J. Phys. Chem. A* **1997**, *101*, 2960−2968.

(4) Leach, S.; Vervloet, M.; Desprès, A.; Bréheret, E.; Hare, J. P.; Denniss, T. J.; Kroto, H. W.; Taylor, R.; Walton, D. R. M. *Chem. Phys.* **1992**, *160*, 451−466.

(5) Negri, F.; Orlandi, G.; Zerbetto, F. *Chem. Phys. Lett.* **1988**, *144*, 31−37.
(6) Yabana, K.; Bertsch, G. F. *Chem. Phys. Lett.* **1992**, *197*, 32−37.
(7) Muramatsu, S.; Nasu, K.; Takahashi, M.; Kaya, K. *Chem. Phys. Lett.* **1977**, *50*, 284−288.
(8) Shelnutt, J. A.; Cheung, L. D.; Chang, R. C. C.; Yu, N.-T.; Felton, R. H. *J. Chem. Phys.* **1977**, *66*, 3387−3397.
(9) Gallagher, S. H.; Armstrong, R. S.; Lay, P. A.; Reed, C. A. *J. Phys. Chem.* **1995**, *99*, 5817−5825.
(10) Margadonna, S.; Prassides, K. J. *Solid State Chem.* **2002**, *168*, 639−652.
(11) Sawamura, M.; Kawai, K.; Matsuo, Y.; Kanie, K.; Kato, T.; Nakamura, E. *Nature* **2002**, *419*, 702−705.
(12) Love, S. P.; McBranch, D.; Salkola, M. I.; Coppa, N. V.; Robinson, J. M.; Swanson, B. I.; Bishop, A. R. *Chem. Phys. Lett.* **1994**, *225*, 170−180.
(13) Rubstov, I. V.; Khudiakov, V. A.; Nadtochenko, A. S.; Lobach, A. S.; Moravskii, A. P. *Chem. Phys. Lett.* **1994**, *229*, 517−523.
(14) Gallagher, S. H.; Ph.D. Thesis, University of Sydney, 1996.
(15) Bauernscmitt, R.; Ahlrichs, R.; Hennrich, F. H.; Kappes, M. M. *J. Am. Chem. Soc.* **1998**, *120*, 5052−5059.
(16) Shelnutt, J. A. *J. Chem. Phys.* **1980**, *72*, 3948−3958.
(17) Opus/LT Spectroscopic Software; 3.1 ed.; Bruker, 2000.
(18) Chambers, G.; Byrne, H. J. *Chem. Phys. Lett.* **1999**, *302*, 307−311.
(19) Lebedken, S.; Gromov, A.; Giesa, S.; Gleiter, R.; Renker, B.; Rietschel, H.; Kratschmer, W. *Chem. Phys. Lett.* **1998**, *285*, 210−215.
(20) Krause, M.; Dunsch, L.; Seifert, G.; Fowler, P. W.; Gromov, A.; Kratschmer, W.; Gutierez, R.; Porezag, D.; Frauenheim, T. *J. Chem. Soc., Faraday Trans.* **1998**, *94*, 2287−2294.
(21) Ying, Q.; Marecek, J.; Chu, B. *J. Chem. Phys.* **1994**, *101*, 2665−2671.
(22) Rudalevige, T.; Francis, A. H.; Zand, R. *J. Phys. Chem. A* **1998**, *102*, 9797−9802.
(23) Nath, S.; Pal, H.; Sapre, A. V. *Chem. Phys. Lett.* **2000**, *327*, 143−148.
(24) Choi, C. H.; Kertesz, M.; Mihaly, L. *J. Phys. Chem. A* **2000**, *104*, 102−112.
(25) Hara, T.; Onoe, J.; Takeuchi, K. *Phys. Rev. B* **2001**, *63*, 115412.
(26) Schettino, V.; Pagliai, M.; Ciabini, L.; Cardini, G. *J. Phys. Chem. A* **2001**, *105*, 11192−11196.
(27) Coulombeau, C.; Jobic, H.; Bernier, P.; Fabre, C.; Schultz, D.; Rassat, A. *J. Phys. Chem. A* **1992**, *96*, 22−24.
(28) Lynch, K.; Tanke, C.; Menzel, F.; Brockner, W.; Scharff, P.; Stumpp, E. *J. Phys. Chem. A* **1995**, *99*, 7985−7992.
(29) Martin, M. C.; Du, X.; Kwon, J.; Mihaly, L. *Phys. Rev. B* **1994**, *50*, 173−183.
(30) Talyzin, A.; Jansson, U. *J. Phys. Chem. B* **2000**, *104*, 5064−5071.
(31) Kee-Chan, K.; Hauke, F.; Hirsch, A.; Boyd, P. D. W.; Carter, E.; Armstrong, R. S.; Lay, P. A.; Reed, C. A. *J. Am. Chem. Soc.* **2003**, *125*, 4024−4025.
(32) Chen, X. H.; Taga, S.; Iwasa, Y. *Phys. Rev. B* **1999**, *60*, 4351−4356.
(33) Winter, J.; Kuzmany, H. *Phys. Rev. B* **1996**, *53*, 655−661.
(34) Garrell, R. L.; Herne, T. M.; Szafranski, C. A.; Diederich, F.; Ettl, F.; Whetten, R. L. *J. Am. Chem. Soc.* **1991**, *113*, 6302−6303.
(35) Chen, F.; Ph.D. Thesis, University of Sydney, 2002.
(36) Clark, R. J. H.; Stewart, B. *Struct. Bond. (Berlin)* **1979**, *36*, 1−80.
(37) Onida, G.; Andreoni, W.; Kohanoff, J.; Parrinello, M. *Chem. Phys. Lett.* **1994**, *219*, 1−7.
(38) Gallagher, S. H.; Armstrong, R. S.; Bolskar, R. D.; Lay, P. A.; Reed, C. A. *J. Am. Chem. Soc.* **1997**, *119*, 4263−4271.
(39) Clark, R. J. H.; Dines, T. J. *Angew. Chem., Int. Ed. Engl.* **1986**, *25*, 131−158.
(40) Dunn, J. L., private conversation, May 2003.